

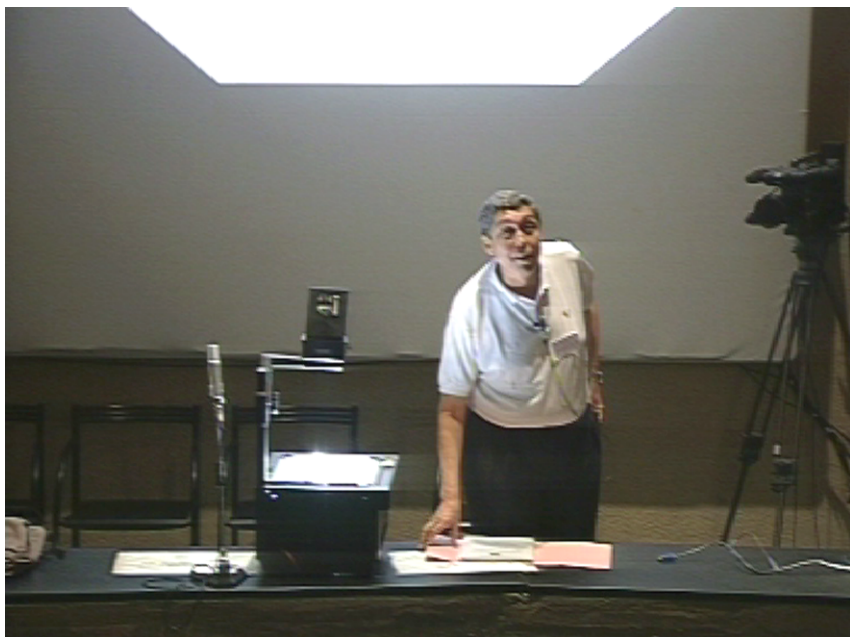
---

# Dipolar Fluctuations in the Bulk and at Interfaces

V. Ballenegger<sup>1</sup>, R. Blaak<sup>2</sup>, and J.-P. Hansen<sup>2</sup>

<sup>1</sup> Laboratoire de Physique Moléculaire, UMR CNRS 6624, Université de Franche-Comté, La Bouloie, 25030 Besançon cedex, France

<sup>2</sup> Department of Chemistry, Lensfield Road, Cambridge CB2 1EW, United Kingdom



Jean-Pierre Hansen

<b>1</b>	<b>Polar Fluids: A Closed Chapter?</b> .....	47
<b>2</b>	<b>Bulk Behaviour of Point and Extended Dipole Molecules</b> .....	48
<b>3</b>	<b>Dipolar Fluctuations in Confined Fluids</b> .....	51
<b>4</b>	<b>Slab Geometry</b> .....	54
<b>5</b>	<b>Spherical Geometry</b> .....	56
<b>6</b>	<b>Polarisation Effects</b> .....	58
<b>7</b>	<b>Summary and Outlook</b> .....	60
	<b>References</b> .....	61

The dielectric response of classical polar fluids is by now well understood for bulk systems, where the permittivity can be calculated by a variety of methods within the linear response regime. Near interfaces or inhomogeneities, one may attempt to describe the dielectric response of the fluid using a local dielectric tensor  $\epsilon(\mathbf{r})$ , for which an explicit expression can be derived from linear response theory. This chapter describes the limitations of this approach, exemplified by Molecular Dynamics simulations of polar fluids confined to a slit or a spherical cavity.

## 1 Polar Fluids: A Closed Chapter?

Many solvents are made up of highly polar molecules, water being the foremost, although somewhat atypical example (due to its hydrogen bonding capacity). Hence it is hardly surprising that a large body of theoretical work has gone into the understanding of polar liquids, and in particular of their dielectric response [1]. Although polar molecules are invariably non-spherical, much insight has been gained from integral equation theories [2] and simulations [3] of simple models involving spherical particles (e.g. hard spheres or Lennard–Jones particles) with an embedded point dipole, the Stockmayer potential being a much studied example. While this field was very active in the eighties and early nineties, it has slowed down since, giving the false impression that everything is well understood. This chapter addresses two open problems, which have only very recently received some attention:

- (a) The point dipole limit is a valid approximation only for intermolecular distances significantly larger than their size. At shorter range, details of the molecular charge distribution become crucially important, as illustrated by the standard models for water (TIP5P, SPC/E, etc.). Hence it is of fundamental interest to investigate models with extended dipoles (constructed from two opposite charges separated by a finite distance  $d$ ) and to determine how, for a given dipole moment, the extension  $d$  affects the dielectric properties and phase behaviour of dense polar fluids, compared to the point dipole limit.
- (b) While the relation between the dielectric permittivity  $\epsilon$  and dipolar fluctuations is well understood in bulk, virtually nothing is known about such fluctuations near an interface between a fluid and a dielectric medium mimicking e.g. a substrate, an electrode, or a membrane. In particular, is it legitimate to define a local permittivity  $\epsilon(\mathbf{r})$  on a nanometric scale, and how is such a profile related to local fluctuations of the dipole moment?

This is of key importance for large-scale biomolecular simulations based on an implicit solvent assumption. The present chapter summarises some of the partial answers to these two open questions which we obtained recently [4–8].

## 2 Bulk Behaviour of Point and Extended Dipole Molecules

We consider spherical molecules carrying extended dipoles consisting of two opposite charges  $\pm q$ , displaced symmetrically by a distance  $d/2$  from the centre of the molecule, such that the absolute dipole moment is  $\mu = qd$ . Obviously the intramolecular charge distribution  $\rho(\mathbf{r}) = q[\delta(\mathbf{r} + \mathbf{d}/2) - \delta(\mathbf{r} - \mathbf{d}/2)]$  will give rise to higher order multipole moments, starting with an octopole.

Only in the limit  $q \rightarrow \infty$  and  $d \rightarrow 0$  for fixed  $\mu$  (point dipole) will the electrostatic interaction between the molecules reduce to the familiar point dipole interaction:

$$v_{\mu,\mu}(1, 2) = (\boldsymbol{\mu}_1 \cdot \nabla_1)(\boldsymbol{\mu}_2 \cdot \nabla_2)G(\mathbf{r}_1, \mathbf{r}_2) \quad (1)$$

where the Green's function  $G(\mathbf{r}_1, \mathbf{r}_2)$  is the solution of Poisson's equation for a unit charge, subject to appropriate boundary conditions dictated by the surrounding media; for an unbounded system  $G(\mathbf{r}_1, \mathbf{r}_2)$  reduces to the Coulomb potential  $1/|\mathbf{r}_1 - \mathbf{r}_2|$ .

In view of the fact that intramolecular charge distributions are always extended, we examined how the dipole extension, characterised by the ratio  $d/\sigma$  (where  $\sigma$  is the molecular diameter) affects the structural and dielectric properties of a dense polar fluid, for a fixed dipole moment  $\mu$ . The question was investigated in some details by extensive Molecular Dynamics (MD) simulations reported in [6]. The polar molecules interact via a Lennard-Jones potential or a short-range soft-core potential  $v_0(r) = 4u(\sigma/r)^{12}$ , plus the long-range Coulomb interaction due to the two point charges  $\pm q$  separated by a distance  $d$  inside each molecule.

The Hamiltonian of the system of  $N$  molecules is, under periodic boundary conditions, whereby the periodic replications of the basic arbitrary simulation cell of length  $L$  form an infinite sphere, which is itself embedded in an infinite region of permittivity  $\epsilon'$ :

$$H = \sum_{i < j} [v_0(r_{ij}) + q_i q_j \psi(r_{ij})] - \frac{\kappa}{\sqrt{\pi}} \sum_{i=1}^N q_i^2 + \frac{2\pi|\mathbf{M}|^2}{(2\epsilon' + 1)L^3} \quad (2)$$

where  $\mathbf{M} = \sum_{i=1}^N q_i \mathbf{r}_i$  is the total dipole moment of the sample and  $\psi(r_{ij})$  is the usual Ewald sum over Coulombic interactions between two charges and their periodic images;  $\kappa$  is the inverse convergence length used in the Ewald summation [9].

The pair structure can be characterised either by site-site correlation functions  $h_{++}(r) = h_{--}(r)$  and  $h_{+-}(r)$ , or by the molecular pair correlation function  $h(1, 2) = h(\mathbf{r}, \hat{\boldsymbol{\mu}}_1, \hat{\boldsymbol{\mu}}_2)$ , which can be expanded in rotational invariants [10]:

$$h(1, 2) = h^{000}(r) + h^{110}(r)\Phi^{110}(1, 2) + h^{112}(r)\Phi^{112}(1, 2) + \dots \quad (3)$$

where

$$\Phi^{110}(1, 2) = \hat{\boldsymbol{\mu}}_1 \cdot \hat{\boldsymbol{\mu}}_2 \quad (4a)$$

$$\Phi^{112}(1, 2) = 3(\hat{\boldsymbol{\mu}}_1 \cdot \hat{\mathbf{r}})(\hat{\boldsymbol{\mu}}_2 \cdot \hat{\mathbf{r}}) - \hat{\boldsymbol{\mu}}_1 \cdot \hat{\boldsymbol{\mu}}_2 \quad (4b)$$

The bulk permittivity  $\epsilon$  of the fluid may be determined by one of the following five routes (not mentioning applied field simulations):

- (a) Via Kirkwood's fluctuation formula [11]

$$\begin{aligned} \frac{(\epsilon - 1)(2\epsilon' + 1)}{2\epsilon' + \epsilon} &= \frac{4\pi}{3V} \frac{\langle |\mathbf{M}|^2 \rangle}{k_B T} \\ &= 3yg_\kappa \end{aligned} \quad (5)$$

valid for a macroscopic spherical sample of volume  $V$  embedded in a medium of permittivity  $\epsilon'$ ;  $y$  is the dimensionless parameter  $4\pi\beta\rho\mu^2/9$  (with  $\rho = N/V$  and  $\beta = 1/k_B T$ ), while  $g_\kappa = \langle |\mathbf{M}|^2 \rangle / N\mu^2$  is the Kirkwood "g-factor", a measure of the orientational correlations between neighbouring dipoles. Onsager's celebrated result is recovered if correlations are neglected, such that  $g_\kappa = 1$ . The correct use of the Kirkwood's formula (5) in simulations, in conjunction with periodic boundary conditions (Ewald summations or Reaction Field), was clarified by Neumann [12]. It is obvious from (5) that the g-factor depends on the dielectric constant  $\epsilon'$  around the macroscopic sample. The  $\epsilon$  derived from (5) can however be shown to be independent of this boundary condition, both theoretically for an arbitrary sample shape [13, 14], as well as in simulations performed in periodic boundary conditions. Kirkwood's formula (5) results from a simple linear response analysis which will be generalised to the inhomogeneous case in Sect. 3.

- (b) A variant of route *a* is obtained by expliciting the Kirkwood "g-factor" in terms of the projection  $h^{110}(r)$  of the pair distribution function (3):

$$\begin{aligned} g_\kappa &= 1 + \sum_{i \neq j} \frac{\langle \boldsymbol{\mu}_i \cdot \boldsymbol{\mu}_j \rangle}{N\mu^2} \\ &= 1 + \frac{4\pi\rho}{3} \int h_{\epsilon'}^{110}(r)r^2 dr \end{aligned} \quad (6)$$

where  $h^{110}$  depends sensitively on the permittivity  $\epsilon'$  of the embedding medium [6, 15].

- (c) The projection  $h^{112}(r)$  is related to  $\epsilon$  by its asymptotic limit [16] which is independent of  $\epsilon'$  for sufficiently large samples:

$$\lim_{r \rightarrow \infty} r^3 h^{112}(r) = \frac{(\epsilon - 1)^2}{\epsilon} \frac{1}{4\pi\rho y} \quad (7)$$

Thus  $\epsilon$  might also be extracted from Monte Carlo (MC) or MD data for  $h^{112}(r)$ , provided the sample is large enough for this projection to reach the asymptotic limit.

- (d) In the case of extended (as opposed to point) dipoles,  $\epsilon$  may also be calculated, in principle, from the Stillinger–Lovett perfect screening condition, valid for an ionic system [17–19].

The total charge-charge correlation function has intra and intermolecular contributions:

$$\begin{aligned} S(r) &= S_{\text{intra}}(r) + S_{\text{inter}}(r) \\ &= \left[ 2q^2 \rho \delta(\mathbf{r}) - 2q^2 \rho \frac{\delta(|\mathbf{r}| - d)}{4\pi d^2} \right] + 2q^2 \rho^2 [h_{++}(r) - h_{--}(r)] \end{aligned} \quad (8)$$

The second Stillinger–Lovett (or perfect screening) condition reads:

$$\frac{1 - \epsilon}{\epsilon} = \frac{2\pi\beta}{3} \int r^2 S(r) d\mathbf{r} \quad (9)$$

This route is in practice of little use for highly polar systems ( $\epsilon \gg 1$ ), because of the unfavourable ratio  $(1 - \epsilon)/\epsilon$ , which would require extremely accurate determinations of  $S(r)$ .

- (e) For completeness, we mention finally Ramshaw’s formula [13] which expresses the dielectric constant as an integral over the direct correlation function:

$$\frac{\epsilon - 1}{\epsilon + 2} = y \left[ 1 - \frac{\rho}{16\pi^2} \int d\mathbf{r} \int d\hat{\boldsymbol{\mu}}_1 \int d\hat{\boldsymbol{\mu}}_2 c(\mathbf{r}, \hat{\boldsymbol{\mu}}_1, \hat{\boldsymbol{\mu}}_2) \hat{\boldsymbol{\mu}}_1 \cdot \hat{\boldsymbol{\mu}}_2 \right]^{-1} \quad (10)$$

where the molecular direct correlation function  $c$  is related to the molecular pair correlation function  $h$  by the Ornstein–Zernike relation [2, 10]:

$$\begin{aligned} h(\mathbf{r}_1, \hat{\boldsymbol{\mu}}_1, \mathbf{r}_2, \hat{\boldsymbol{\mu}}_2) &= c(\mathbf{r}_1, \hat{\boldsymbol{\mu}}_1, \mathbf{r}_2, \hat{\boldsymbol{\mu}}_2) \\ &\quad + \rho \int d\mathbf{r}_3 \int d\hat{\boldsymbol{\mu}}_3 c(\mathbf{r}_1, \hat{\boldsymbol{\mu}}_1, \mathbf{r}_3, \hat{\boldsymbol{\mu}}_3) h(\mathbf{r}_3, \hat{\boldsymbol{\mu}}_3, \mathbf{r}_2, \hat{\boldsymbol{\mu}}_2) \end{aligned} \quad (11)$$

Route  $c$  yields accurate values of  $\epsilon$ , provided a sufficiently large system is simulated for  $h^{112}(r)$  to reach its asymptotic value. A similar requirement holds for route  $b$ , while route  $a$  can be used with smaller systems. An error analysis [6] shows that the choice of metallic boundary conditions at infinity ( $\epsilon' = \infty$ ) is optimal in the sense that it minimises the uncertainty in  $\epsilon$  for a given simulation time. The convergence with the number of timesteps is slow, because  $\epsilon$  is related to fluctuations of the total dipole moment  $\mathbf{M}$  around its mean  $\langle \mathbf{M} \rangle = 0$ . This is illustrated in Fig. 1 which shows that simulation times of several nanoseconds are required to arrive at a 5% accuracy.

The “sluggishness” of the convergence may be traced back to the slow decay of the autocorrelation function of the total dipole moment  $\mathbf{M}(t)$ . At liquid densities, the relaxation is essentially exponential with a relaxation time  $\tau_M$  of typically 10 ps, an order of magnitude larger than the time associated

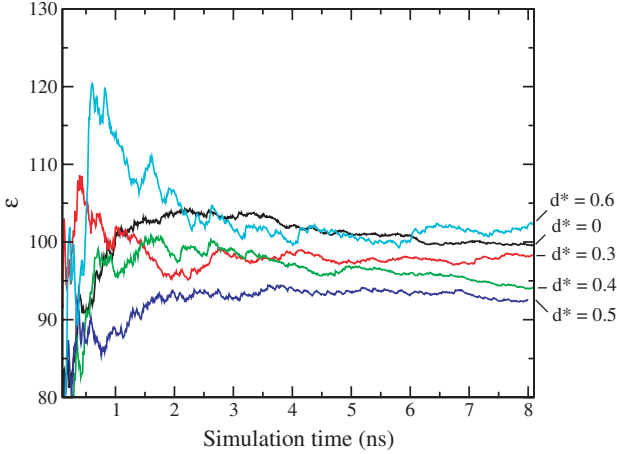


**Fig. 1.** Convergence of  $\epsilon$  with simulation time, for dipole elongations  $d^* = d/\sigma = 0, 0.3, 0.4, 0.5$  and  $0.6$ . (After Ballenegger and Hansen [6])

with the single dipole relaxation, which follows a stretched exponential behaviour [6]. Note that  $\tau_M$  increases with the elongation of  $d/\sigma$ , due to the enhanced tendency towards alignment (string formation) of the dipoles.

Comparing results for different elongations (but the same  $\mu$ ) shows that the extended dipole results begin to deviate from the point dipole data only for  $d/\sigma \gtrsim 0.3$ . As the ratio increases further, the dipolar molecules tend to form head-to-tail strings, and the polar fluid undergoes a transition to a hexagonal columnar phase [6], which occurs for much lower values of  $\mu$  compared to the point dipole case [20, 21].

### 3 Dipolar Fluctuations in Confined Fluids

We now turn to the largely uncharted territory of the dielectric behaviour of confined polar fluids near dielectric interfaces. The general geometry is sketched in Fig. 2:  $N$  dipolar molecules are confined to a cavity of arbitrary shape carved out of a medium of macroscopic dielectric permittivity  $\epsilon'$ . Two situations will be considered:

- (a)  $\epsilon' = 1$ , i.e. the confining medium is non polarisable; in that case the dielectric behaviour of the fluid is modified due to the geometric confinement only.
- (b)  $\epsilon' > 1$ , then the dielectric behaviour is affected both by geometric confinement and by the polarisation of the confining medium. Polarisation effects introduce boundary conditions at the interfaces, which can be handled either by the method of images [22], which is useful only for very simple geometries, or by a variational method based on the optimisation of

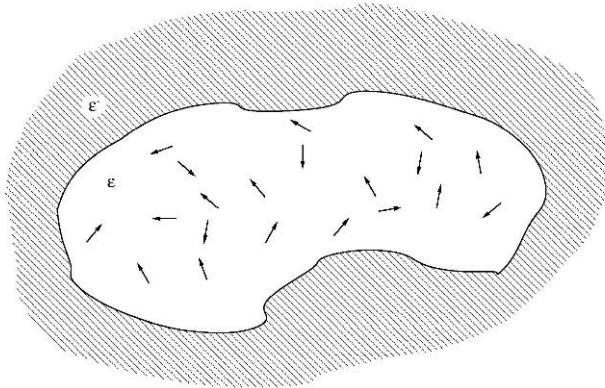


**Fig. 2.** Sketch of dipoles confined to a cavity embedded in a dielectric medium  $\epsilon'$

an appropriate functional with respect to the surface polarisation charge density [23–25].

The two key questions to be asked concerning the dielectric response of a polar fluid near a confining surface are the following:

- (a) Is there a local, linear relationship between the induced mean polarisation density  $\mathbf{P}(\mathbf{r})$  and the local (Maxwell) electric field  $\mathbf{E}(\mathbf{r})$  of a form generalising the standard macroscopic expression [22], i.e.:

$$\mathbf{P}(\mathbf{r}) = \frac{\epsilon(\mathbf{r}) - 1}{4\pi} \mathbf{E}(\mathbf{r}) \quad (12)$$

where  $\epsilon(\mathbf{r})$  is a local permittivity tensor (which reduces to a constant scalar in the bulk of an isotropic fluid)?

- (b) If such a relation holds (at least for sufficiently weak applied field), what is the microscopic expression for  $\epsilon(\mathbf{r})$ , which generalises Kirkwood's relation (5)?

The limits of validity of the local relation (12) are discussed in references [5] and [16]. Roughly speaking a local relation holds provided the field does not vary appreciably over the range of the bulk pair correlation function. A general formal expression for  $\epsilon(\mathbf{r})$  was derived in [5]. Expressions for specific, simple geometries will be given below.

The simplest geometry is a semi-infinite system confined (say to  $z > 0$ ) by a plane ( $z = 0$ ) and a dielectric medium  $\epsilon'$  extending to negative  $z$ . Under these conditions the dielectric permittivity tensor, if it exists, is necessarily of the form:

$$\epsilon(z) = \begin{pmatrix} \epsilon_{\parallel}(z) & 0 & 0 \\ 0 & \epsilon_{\parallel}(z) & 0 \\ 0 & 0 & \epsilon_{\perp}(z) \end{pmatrix} \quad (13)$$

Exact expressions for  $\epsilon_{\parallel}(z)$  and  $\epsilon_{\perp}(z)$  in the asymptotic region close to the bulk limit may be derived and exhibit a  $1/z^3$  variation [5]; the same is true of the anisotropic one-particle density  $\rho(z, \theta)$  (where  $\theta$  is the angle between a dipole and the  $z$  axis) [26]. Direct simulation of such a semi-infinite polar fluid is not possible, because periodic boundary conditions cannot be satisfied in the  $z$ -direction. Periodicity can only be achieved for a slab of polar fluid confined between two dielectric slabs, which may mimic, for instance, membranes or clay platelets.

As in the case of bulk polar fluids, the general procedure to derive a microscopic expression for the local permittivity  $\epsilon(\mathbf{r})$  of a confined fluid is based on a linear response argument [1, 7, 27]. This proceeds in two steps: first the induced polarisation of the sample is related to the cavity field  $\mathbf{E}^c$ , i.e. the field created inside the *empty* cavity by an external field  $\mathbf{E}'$ . The second step is to relate the Maxwell field inside the *filled* cavity to the cavity field;  $\epsilon(\mathbf{r})$  then follows from the definition (12). The first step may be formally carried out for a cavity of arbitrary shape. Let  $\mathbf{m}(\mathbf{r})$  be the microscopic polarisation density:

$$\mathbf{m}(\mathbf{r}) = \sum_{i=1}^N \boldsymbol{\mu}_i \delta(\mathbf{r} - \mathbf{r}_i) \quad (14)$$

where  $\mathbf{r}_i$  and  $\boldsymbol{\mu}_i$  are the centre of mass position and dipole moment of the  $i$ th molecule ( $1 \leq i \leq N$ ). The total dipole moment of the sample is:

$$\mathbf{M} = \int_{\text{cavity}} \mathbf{m}(\mathbf{r}) d\mathbf{r} \quad (15)$$

The mean local polarisation density is the statistical average of (14). Let  $\mathbf{E}'$  be a uniform externally applied field in the confining dielectric, far from the cavity. The induced polarisation density is:

$$\begin{aligned} \Delta \mathbf{P}(\mathbf{r}) &= \mathbf{P}(\mathbf{r}) - \mathbf{P}_0(\mathbf{r}) \\ &= \langle \mathbf{m}(\mathbf{r}) \rangle_{\mathbf{E}'} - \langle \mathbf{m}(\mathbf{r}) \rangle \end{aligned} \quad (16)$$

where the two terms are the polarisations in the presence and absence ( $\mathbf{P}_0(\mathbf{r})$ ) of external field. In many situations symmetry implies that  $\mathbf{P}_0(\mathbf{r}) = 0$ . The general relation between  $\Delta \mathbf{P}$  and the corresponding difference in Maxwell fields  $\Delta \mathbf{E}(\mathbf{r}) = \mathbf{E}(\mathbf{r}) - \mathbf{E}_0(\mathbf{r})$  is:

$$\Delta \mathbf{P}(\mathbf{r}) = \frac{1}{4\pi} \int_{\text{cavity}} \chi(\mathbf{r}, \mathbf{r}') \cdot \Delta \mathbf{E}(\mathbf{r}') d\mathbf{r}' \quad (17)$$

which reduces to (12) if a local relation  $\chi(\mathbf{r}, \mathbf{r}') = \chi(\mathbf{r}) \delta(\mathbf{r} - \mathbf{r}') = (\epsilon(\mathbf{r}) - 1) \delta(\mathbf{r} - \mathbf{r}')$  holds and if  $\mathbf{E}_0(\mathbf{r}) = 0$  by symmetry. Expliciting the statistical average  $\langle \mathbf{m}(\mathbf{r}) \rangle_{\mathbf{E}'}$  in (16) we arrive at:

$$\Delta \mathbf{P}(\mathbf{r}) = \frac{\int [\mathbf{m}(\mathbf{r}) - \langle \mathbf{m}(\mathbf{r}) \rangle] \exp \{-\beta [U_{\epsilon'}(1, \dots, N) - \mathbf{M} \cdot \mathbf{E}^c]\} d1 \dots dN}{\int \exp \{-\beta [U_{\epsilon'}(1, \dots, N) - \mathbf{M} \cdot \mathbf{E}^c]\} d1 \dots dN} \quad (18)$$

where  $di = d\mathbf{r}_i d\hat{\boldsymbol{\mu}}_i$ ,  $U_{\epsilon'}$  is the total interaction energy of  $N$  dipolar molecules within the cavity embedded in the dielectric  $\epsilon'$ , while the total dipole moment is coupled to the cavity (rather than the external) field.

Linearisation of the Boltzmann factors with respect to  $\mathbf{E}^c$  immediately leads to the linear response result:

$$\Delta \mathbf{P}_\alpha(\mathbf{r}) = \beta \sum_{\gamma=x,y,z} [\langle m_\alpha(\mathbf{r}) M_\gamma \rangle - \langle m_\alpha(\mathbf{r}) \rangle \langle M_\gamma \rangle] E_\gamma \quad (19)$$

where the statistical averages are to be taken over the unperturbed system (i.e. for  $\mathbf{E}' = 0$ ).

The next task is to relate  $\mathbf{E}^c$  to  $\mathbf{E}$ ; this depends on the geometry of the cavity and the permittivity  $\epsilon'$ . In Sect. 4 we consider the slab geometry, while the case of a spherical cavity will be examined in Sects. 5 and 6.

## 4 Slab Geometry

The ‘‘cavity’’ reduces to an infinite slab in the  $x$  and  $y$  directions, confined between two semi-infinite dielectric media  $\epsilon'$ . The interfaces are planes orthogonal to  $z$ . The local dielectric tensor is of the form (13). By symmetry, the component of  $\mathbf{P}$  parallel to the planes vanishes in the absence of an external field, so that (12) splits into:

$$\mathbf{P}_\parallel(z) = \frac{\epsilon_\parallel(z) - 1}{4\pi} \mathbf{E}_\parallel(z) \quad (20a)$$

$$P_\perp(z) = \frac{\epsilon_\perp(z) - 1}{4\pi} E_\perp(z) \quad (20b)$$

where all vectors with the subscript  $\parallel$  are 2d vectors in the  $x$ - $y$  plane.

The standard electrostatic boundary conditions relate the cavity to the external field, i.e.:

$$\begin{aligned} \mathbf{E}_\parallel^c &= \mathbf{E}'_\parallel \\ \mathbf{E}_\perp^c &= \epsilon' \mathbf{E}'_\perp \end{aligned} \quad (21)$$

Maxwell’s equation  $\nabla \wedge \mathbf{E}(z) = 0$  shows that  $\mathbf{E}_\parallel$  is independent of  $z$  and hence  $\mathbf{E}_\parallel = \mathbf{E}'_\parallel$  everywhere. Remembering (20a), we conclude that:

$$\mathbf{P}_\parallel(z) = \frac{\epsilon_\parallel(z) - 1}{4\pi} \mathbf{E}_\parallel^c \quad (22)$$

Equations (19) and (22), together with the isotropy in the  $x$ - $y$  plane then imply the following generalised Kirkwood relation for  $\epsilon_\parallel(z)$ :

$$\epsilon_{\parallel}(z) = 1 + 2\pi\beta [\langle \mathbf{m}_{\parallel}(z) \cdot \mathbf{M}_{\parallel} \rangle - \langle \mathbf{m}_{\parallel}(z) \rangle \cdot \langle \mathbf{M}_{\parallel} \rangle] \quad (23)$$

Note that the dipolar density at  $z$  must be correlated not with itself (as one might naively have guessed) but with the total dipole moment of the slab.

A similar calculation, now using the Maxwell relation  $\nabla \cdot \mathbf{D}(z) = 0$  (with  $\mathbf{D} = \mathbf{E} + 4\pi\mathbf{P}$ ), leads to the following expression for  $\epsilon_{\perp}(z)$  [7]:

$$\frac{\epsilon_{\perp}(z) - 1}{\epsilon_{\perp}(z)} = 1 + 2\pi\beta [\langle m_{\perp}(z) M_{\perp} \rangle - \langle m_{\perp}(z) \rangle \langle M_{\perp} \rangle] \quad (24)$$

One immediately notes that the unfavourable ratio on the left hand side will make it very difficult to extract accurate values of  $\epsilon_{\perp}(z)$  from simulation estimates of the fluctuations on the right hand side.

A first attempt to extract  $\epsilon_{\parallel}(z)$  and  $\epsilon_{\perp}(z)$  from MD simulations was made in [7], for a system of “soft spheres” (short-range pair interactions  $v(r) = 4u(\sigma/r)^{12}$ ) with extended dipoles ( $d/\sigma = 1/3$ ), confined to a slab of width  $L$ , surrounded on both sides by vacuum ( $\epsilon' = 1$ ). The electrostatic interaction of a periodic array of such slabs can be handled by 3d Ewald summations with a dipole layer correction term [28–30].  $\epsilon_{\parallel}(z)$  and  $\epsilon_{\perp}(z)$  can be computed from the fluctuation formulae (23) and (24), or by applying a uniform external field  $\mathbf{E}'$  parallel (for  $\epsilon_{\parallel}$ ) or perpendicular (for  $\epsilon_{\perp}$ ) to the slab. In the parallel case a measurement of  $\mathbf{P}_{\parallel}(z)$  then directly determines  $\epsilon_{\parallel}(z)$  via (22), since  $\mathbf{E}_{\parallel}^c = \mathbf{E}'_{\parallel}$ .  $\epsilon_{\perp}(z)$  may also be estimated in a similar way [7]. Results for  $\epsilon_{\parallel}(z)$  and two different dipole moments are plotted in Fig 3. The two

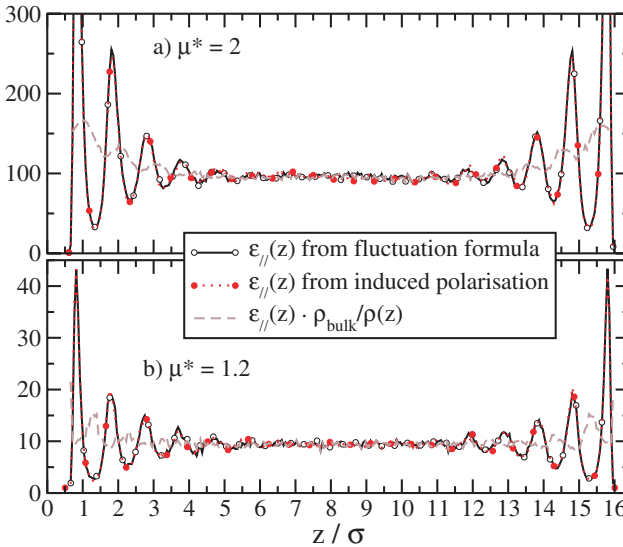


**Fig. 3.** Parallel component of the permittivity tensor from fluctuation formula (23) and from the response to an external field  $E' = 0.1$  V/nm along the  $x$  axis. (Reused with permission from [7]. Copyright 2005, American Institute of Physics)

estimates of  $\epsilon_{\parallel}(z)$  based on (22) and (23) are in excellent agreement. The pronounced oscillations of  $\epsilon_{\parallel}(z)$  near the two interfaces are intimately correlated with the oscillations in the density profile  $\rho(z)$ , which reflect the layering of the dipolar spheres near the walls, as is clear from the plots of  $\epsilon_{\parallel}(z)\rho_{\text{bulk}}/\rho(z)$ , where  $\rho_{\text{bulk}}$  is the bulk density of the fluid, reached half-way between the two plates where  $\epsilon(z)$  tends to its bulk value. The behaviour of the “envelope”  $\epsilon_{\parallel}(z)\rho_{\text{bulk}}/\rho(z)$  near the interfaces suggests that on a suitably coarse-grained scale,  $\epsilon(z)$  tends to increase over its bulk value on approaching the dielectric walls. This behaviour may change qualitatively when the dielectric media on both sides of the slab are polarisable ( $\epsilon' > 1$ ) or carry a surface charge; these issues will be addressed in future simulation work.

As anticipated,  $\epsilon_{\perp}(z)$  fails to converge to physically acceptable values, even for very long (several ns) MD runs, except in the bulk region, far from the interfaces, where it tends to the same limit as  $\epsilon_{\parallel}(z)$ .

An unexpected result of the simulations in [7] is the dramatic “overscreening” of an externally applied field by the local polarisation density in the immediate vicinity of the interfaces, where the ratio  $E(z)/E'$  can become very large and negative (typically  $\simeq -2$ ).

The general behaviour described in this section is not specific to dipolar soft spheres, but remains at least qualitatively very similar for SPC/E water confined to a slit [7].

## 5 Spherical Geometry

We next consider a dipolar fluid confined to a spherical cavity of radius  $R$  carved out of a dielectric medium  $\epsilon'$ . The cavity field is now  $\mathbf{E}^c = 3\epsilon'\mathbf{E}'/(2\epsilon'+1)$  [22], and adaptation of the linear response argument of Sect. 3 to this isotropic case leads to

$$\frac{(\epsilon - 1)(2\epsilon' + 1)}{2\epsilon' + \epsilon} = \frac{4\pi\beta}{3V} [\langle \mathbf{m}(\mathbf{r}) \cdot \mathbf{M} \rangle - \langle \mathbf{m}(\mathbf{r}) \rangle \cdot \langle \mathbf{M} \rangle] \quad (25)$$

where  $\mathbf{r}$  can be any point in the bulk of the system, except in the vicinity of the spherical interface. Away from the interface,  $\mathbf{m}(\mathbf{r})$  may hence be replaced by  $\mathbf{M}/V$  so that (25) leads back to Kirkwood’s formula (5) (with  $\langle \mathbf{M} \rangle = 0$ , which in simulations is only achieved for sufficiently long runs).

We now consider the case of a radial, external field due to an “external” charge  $q$  placed at the centre of the cavity filled with polar molecules, so that  $\mathbf{E}'(\mathbf{r}) = q\hat{\mathbf{r}}/r^2$ . In that case the permittivity depends only on the radial distance from the centre, and the linear response argument leads to the microscopic expression [7]:

$$\frac{\epsilon(r) - 1}{\epsilon(r)} = 4\pi\beta \int_{\text{cavity}} \langle m(\mathbf{r})m(\mathbf{r}') \rangle \left(\frac{r}{r'}\right)^2 d\mathbf{r}' \quad (26)$$

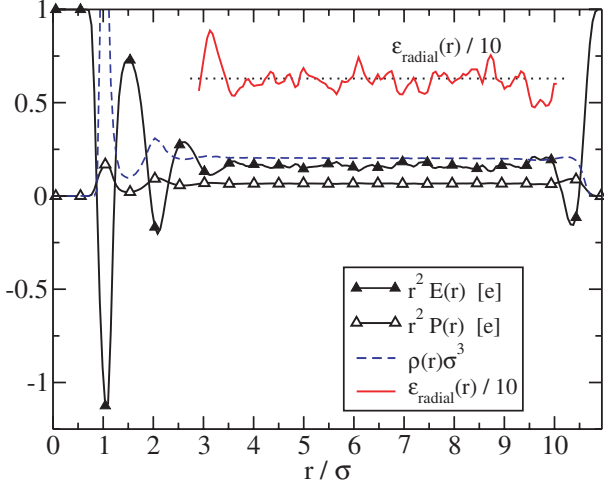


**Fig. 4.** Radial electric field, polarisation density, molecular density, and permittivity profiles for a spherical droplet of polar fluid ( $\mu^* = 2$ ,  $T^* = 1.35$ ,  $\rho^* = 0.2$ ) when an ion of unit electronic charge (reduced charge  $q^* = 28.7$ ) is present at the origin. The *dotted line* indicates the bulk dielectric constant  $\epsilon = 6.3$  (divided by 10). (Reused with permission from [7]. Copyright 2005, American Institute of Physics)

where  $m = \mathbf{m} \cdot \hat{\mathbf{r}}$  is the radial projection of the microscopic polarisation density (14). Note that, contrary to (25), this relation does not depend explicitly on  $\epsilon'$  (but of course implicitly through the Boltzmann weight in the statistical average).

Equation (26) is not very convenient for computational purposes, because of the integration on the right hand side. The local and applied fields are related by the intuitively satisfactory relation [7]

$$E(r) = \frac{E'(r)}{\epsilon(r)} \quad (27)$$

which is a direct consequence of the local assumption (12). The profile  $E(r) = q(r)/r^2$ , where  $q(r) = q - 4\pi r^2 P(r)$  is the charge inside a sphere of radius  $r$  and  $P(r)$  is the radial component of the polarisation density, which may be measured via definition (16) (with  $P_0 = 0$  for linear dipoles). Examples of the various profiles, when an ion of charge  $q^* = q\mu/(\sigma^2 u) = 28.7$  is placed at the origin, are shown in Fig. 4 in the case where  $\epsilon' = 1$ . The resulting  $\epsilon(r)$  is compatible with the bulk value away from the centre and the interface, but is ill-defined as the latter are approached. Note that the “overscreening” effect, observed in the slab geometry, is also very marked near the central charge.

## 6 Polarisation Effects

So far we have carefully avoided the complications due to the polarisation charge induced on the confining surfaces by the dipoles of the confined polar fluid, by assuming  $\epsilon' = 1$  in all simulations. For  $\epsilon' > 1$  electrostatic boundary conditions must be satisfied at the surface separating the confining medium from the atomistically resolved polar fluid, where molecules evolve in vacuo ( $\epsilon = 1$ ). Let  $\mathbf{n}$  be the normal to the surface carrying a surface charge density  $\sigma$  (only the case  $\sigma = 0$  will be considered throughout). The electric fields  $\mathbf{E}'$  and  $\mathbf{E}$  on either side of the surface obey the conditions [22]

$$(\epsilon' \mathbf{E}' - \epsilon \mathbf{E}) \cdot \mathbf{n} = 4\pi\sigma \quad (28a)$$

$$(\mathbf{E}' - \mathbf{E}) \wedge \mathbf{n} = 0 \quad (28b)$$

For sufficiently simple geometries, the solution to Maxwell's equations  $\nabla \wedge \mathbf{E} = 0$  and  $\nabla \cdot (\epsilon \mathbf{E}) = 0$ , subject to the boundary conditions (28) may be conveniently obtained by the introduction of image charges. In the simplest case of a single planar surface separating the two media as depicted in Fig. 5, the electrostatic potential  $\Phi(\mathbf{r})$  inside the medium  $\epsilon$  due to a single charge  $q$  is the sum of the potentials due to that charge and a single image charge  $q' = (\epsilon - \epsilon')q/(\epsilon + \epsilon')$ , positioned at the mirror location with respect to the planar surface, in the absence of the dielectric discontinuity. In the case of the slab geometry used in simulations, an infinite array of images is required to satisfy the boundary conditions. In the case of a spherical cavity the problem turns out to be highly non-trivial [8], except in the case where the confining medium is a metal ( $\epsilon' = \infty$ ) [22]. Referring to Fig. 6, the electrostatic potential at  $\mathbf{r}$  due to a simple charge  $q$  placed at  $\mathbf{d}$  is [8]:

$$\begin{aligned} \Phi(\mathbf{r}) = \frac{q}{4\pi\epsilon} \left\{ \frac{1}{|\mathbf{r} - \mathbf{d}|} + (1 - 2\kappa) \frac{R/d}{|\mathbf{r} - \mathbf{D}|} \right\} \\ + \frac{q(1 - 2\kappa)}{4\pi\epsilon'R} F_1 \left( \kappa, \frac{1}{2}, \frac{1}{2}, 1 + \kappa; x e^{i\theta}, x e^{-i\theta} \right) \end{aligned} \quad (29)$$

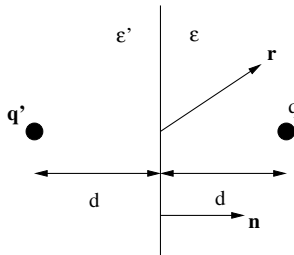


**Fig. 5.** The electrical potential field at  $\mathbf{r}$  due to a single charge  $q$  in the case of a planar interface separating the media  $\epsilon$  and  $\epsilon'$ , is effectively described by the combined contributions of the charge  $q$  and its image  $q'$

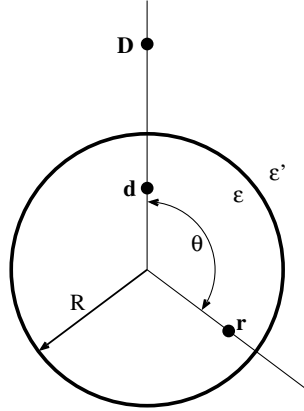


**Fig. 6.** Schematic representation of a charge at position  $\mathbf{d}$  inside a spherical cavity of radius  $R$  and permittivity  $\epsilon$  embedded in an infinite medium  $\epsilon'$

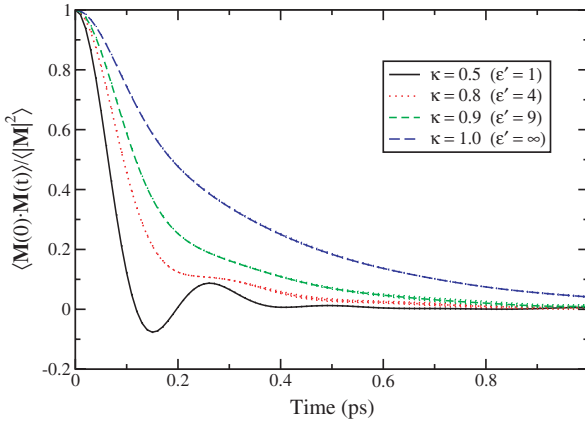


**Fig. 7.** Time correlation function  $\langle \mathbf{M}(0) \cdot \mathbf{M}(t) \rangle$  of the total dipole moment of a polar fluid inside a spherical cavity surrounded by a dielectric medium with  $\epsilon' = 1, 4, 9,$  and  $\infty$  ( $N = 1000, R = 3$  nm)

where  $F_1$  is a hyper-geometric function in the two complex variables  $xe^{i\theta}$  and  $xe^{-i\theta}$ , with  $x = rd/R^2$ ,  $\kappa = \epsilon'/(\epsilon + \epsilon')$ , and  $\mathbf{D} = (R/d)^2 \mathbf{d}$ . The classic result for a cavity inside a metal is recovered when  $\epsilon \rightarrow \infty$  or  $\kappa \rightarrow 1$ .

The dielectric behaviour of a polar fluid trapped inside a spherical cavity is very sensitive to the dielectric permittivity  $\epsilon'$  of the confining medium. This is illustrated in Fig. 7, which shows the correlation function of the total dipole moment  $\mathbf{M}(t)$  of  $N = 1000$  dipolar molecules with  $\mu^* = 2$  trapped inside a cavity of radius  $R = 3$  nm. The oscillatory relaxation observed for  $\epsilon' = 1$  (vacuum) is seen to go over into a very slow relaxation when  $\epsilon' = \infty$ . The slowing down of the relaxation as  $\epsilon'$  increases agrees with the increase

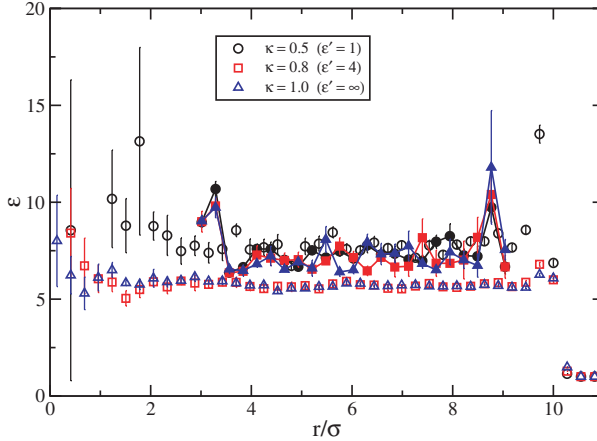


**Fig. 8.** Dielectric profiles  $\epsilon(r)$  inside a spherical cavity, with a radius of 4 nm and 1000 dipoles, surrounded by a dielectric medium with  $\epsilon' = 1, 4$ , and  $\infty$  obtained by the fluctuation formula (25) (*open symbols*) and (non-) linear response (27) (*filled symbols*)

of the Debye relaxation time in bulk dielectrics, predicted by Neumann and Steinhauser [31]. Permittivity profiles,  $\epsilon(r)$ , as estimated, for three values of  $\epsilon'$ , from the fluctuation formula (25), and from the (non-linear) response to a central charge (27) are shown in Fig. 8. In the case  $\epsilon' = 1$ , the linear and non-linear responses are seen to be rather close. For  $\epsilon' = 4$  and  $\epsilon' = \infty$ , the linear profiles are significantly lower than their  $\epsilon' = 1$  counterpart, while the non-linear response profiles appear to be less sensitive to the value of  $\epsilon'$ .

## 7 Summary and Outlook

The main message to be taken away from this chapter is that a microscopic computation of the dielectric response of a polar fluid, and in particular of the dielectric permittivity in the bulk and at interfaces, is still an arduous and non-trivial task, despite several decades of efforts due to the following points:

- (a) The dielectric behaviour of fluids of molecules with extended dipoles closely matches that of point dipoles for extensions  $d/\sigma \lesssim 0.3$ . Dramatic differences appear for  $d/\sigma \gtrsim 0.5$ , due to a stronger tendency towards head-to-tail string formation.
- (b) Kirkwood's fluctuation formula (5) remains the most efficient route to estimating the bulk permittivity  $\epsilon$  by computer simulations, with “metallic” boundary conditions ( $\epsilon' = \infty$ ) at infinity. It must be emphasised, however, that MD trajectories of at least a few ns are required to achieve an accuracy of the order of 5%. Alternative estimates based on the asymptotic

behaviour of partial correlation functions require larger system sizes and tend to be less accurate.

- (c) Assuming a local relation between polarisation and electric field profiles, one can derive generalised fluctuation formulae for the components of a local permittivity tensor  $\epsilon(\mathbf{r})$ . These formulae depend on the geometry of the problem, i.e. on the shape of the confining surface(s), and on the dielectric permittivity  $\epsilon'$  of the confining medium, which is treated as a dielectric continuum. Whenever this medium is polarisable ( $\epsilon' > 1$ ), the dielectric boundary conditions at the confining surface must be accounted for by the method of images (which is tractable for the simplest geometries only), or by a recently developed variational procedure for the calculations of the surface polarisation charge density.

We have shown that in the slab geometry the longitudinal permittivity  $\epsilon_{\parallel}(z)$  appears to be well defined, and strongly influenced by the layering of densely packed polar molecules near the wall. The transverse component  $\epsilon_{\perp}(z)$  is, however, ill-defined and may take on unphysical (negative) values near the walls, thus pointing to the break-down of the assumption of locality.

Preliminary MD data for a polar fluid inside a spherical cavity point to a significant dependence of the dielectric response of the sample to the permittivity  $\epsilon'$  of the confining medium. Although spatially varying local permittivities are being used in implicit solvent simulation of biomolecular assemblies, the conclusion to be drawn from the preliminary results presented in this chapter is that the use of such permittivity profiles on nanoscales is dubious for the least. Moreover the simultaneous use of a fully molecular description of the confined polar fluid, and of a continuum representation of the confining medium (e.g. solid substrates, colloids or membranes) is obviously inconsistent, and introduces artificially sharp dielectric discontinuities at the surfaces. A more satisfactory, but also more computer-intensive model of polar fluids at interfaces would be to use an atomistic representation of the confining medium. We are presently replacing continuous dielectric slabs by polarisable atoms on a lattice. The polarisation of substrate atoms by the charge distribution on the molecules of the polar fluid can be handled by well established, self-consistent methods [32]. The dielectric discontinuity is thus smoothed out over atomistic scales, and a comparison will be made between the dielectric response of a polar fluid near a continuous or atomically resolved substrate.

## References

1. P. A. Madden and D. Kivelson (1984) A consistent molecular treatment of dielectric phenomena. *Adv. Chem. Phys.* **56**, p. 467.
2. J. P. Hansen and I. R. McDonald (1986) *Theory of Simple Liquids*. Academic Press, London, 2nd ed. (Chap. 12)
3. P. G. Kusalik, M. E. Mandy, and I. M. Svishchev (1994) The dielectric constant of polar fluids and the distribution of the total dipolemoment. *J. Chem. Phys.* **100**, p. 7654 (and references therein)

4. R. Finken, V. Ballenegger, and J.-P. Hansen (2003) Onsager model for a variable dielectric permittivity near an interface. *Mol. Phys.* **101**, p. 2559
5. V. Ballenegger and J.-P. Hansen (2003) Local dielectric permittivity near an interface. *Europhys. Lett.* **63**, p. 381
6. V. Ballenegger and J.-P. Hansen (2004) Structure and dielectric properties of polar fluids with extended dipoles: results from numerical simulations. *Mol. Phys.* **102**, p. 599
7. V. Ballenegger and J.-P. Hansen (2005) Dielectric permittivity profiles of confined polar fluids. *J. Chem. Phys.* **122**, p. 114711
8. R. Blaak and J.-P. Hansen (2006) Dielectric response of a polar fluid trapped in a spherical nanocavity. *J. Chem. Phys.* **124**, p. 144714
9. J.-P. Hansen (1986) Molecular-Dynamics Simulation of Coulomb Systems in Two and Three Dimensions. In *Molecular Dynamics Simulation of Statistical Mechanical Systems*. Edited by G. Ciccotti and W. G. Hoover, North-Holland, Amsterdam, Proceedings of the International School of Physics "Enrico Fermi," Course XCVIII, Varenna, 1985, pp. 89–129.
10. C. G. Gray and K. E. Gubbins (1984) *Theory of Molecular Fluids*. vol. 1, Clarendon Press, Oxford
11. J. G. Kirkwood (1939) The dielectric polarization of polar liquids. *J. Chem. Phys.* **7**, p. 911
12. M. Neumann (1983) Dipole moment fluctuation formulas in computer simulations of polar systems. *Mol. Phys.* **50**, p. 841
13. J. D. Ramshaw (1977) Existence of the dielectric constant in rigid dipole fluids: The functional derivative approach. *J. Chem. Phys.* **66**, p. 3134
14. A. Alastuey and V. Ballenegger (2000) Statistical mechanics of dipolar fluids: dielectric constant and sample shape. *Physica A* **279**, p. 268
15. J. M. Caillol (1992) Asymptotic behavior of the pair-correlation function of a polar liquid. *J. Chem. Phys.* **96**, p. 7039
16. G. Nienhuis and J. M. Deutch (1971) Structure of dielectric fluids. I. the two particle distribution function of polar fluids. *J. Chem. Phys.* **55**, p. 4213
17. F. H. Stillinger, Jr. and R. Lovett (1968) Ion-pair theory of concentrated electrolytes. I. basic concepts. *J. Chem. Phys.* **48**, p. 3858
18. R. Lovett and F. H. Stillinger, Jr. (1968) Ion-pair theory of concentrated electrolytes. II. approximate dielectric response calculation. *J. Chem. Phys.* **48**, p. 3869
19. Ph. A. Martin (1988) Sum rules in charged fluids. *Rev. Mod. Phys.* **60**, p. 1075
20. D. Wei and G. N. Patey (1992) Orientational order in simple dipolar liquids: Computer simulation of a ferroelectric nematic phase. *Phys. Rev. Lett.* **68**, p. 2043
21. J. J. Weis, D. Levesque, and G. J. Zarragoicoechea (1992) Orientational order in simple dipolar liquid-crystal models. *Phys. Rev. Lett.* **69**, p. 913
22. J. D. Jackson (1999) *Classical Electrodynamics*. Wiley, New York, 3rd ed.
23. R. Allen, J.-P. Hansen, and S. Melchionna (2001) Electrostatic potential inside ionic solutions confined by dielectrics: a variational approach. *Phys. Chem. Chem. Phys.* **3**, p. 4177
24. R. Allen and J.-P. Hansen (2003) Electrostatic interactions of charges and dipoles near a polarizable membrane. *Mol. Phys.* **101**, p. 1575
25. P. Attard (2003) Variational formulation for the electrostatic potential in dielectric continua. *J. Chem. Phys.* **119**, p. 1365

26. J. P. Badiali (1989) Structure of a polar fluid near a wall, exact asymptotic behavior of the profile, relation with the electrostriction phenomena and the kerr effect. *J. Chem. Phys.* **90**, p. 4401
27. H. A. Stern and S. E. Feller (2003) Calculation of the dielectric permittivity profile for a nonuniform system: Application to a lipid bilayer simulation. *J. Chem. Phys.* **118**, p. 3401
28. I.-C. Yeh and M. L. Berkowitz (1999) Ewald summation for systems with slab geometry. *J. Chem. Phys.* **111**, p. 3155
29. A. Arnold, J. de Joannis, and C. Holm (2002) Electrostatics in periodic slab geometries. *J. Chem. Phys.* **117**, p. 2496
30. J. de Joannis, A. Arnold, and C. Holm (2002) Electrostatics in periodic slab geometries. *J. Chem. Phys.* **117**, p. 2503
31. M. Neumann and O. Steinhauser (1983) On the calculation of the frequency-dependent dielectric constant in computer simulations. *Chem. Phys. Lett.* **102**, p. 508
32. G. Lamoureux and B. Roux (2003) Modeling induced polarization with classical drude oscillators: Theory and molecular dynamics simulation algorithm. *J. Chem. Phys.* **119**, p. 3025 (and references therein)